In Vitro Studies of DNA Damage Caused by Tricyclic Antidepressants: A Role of Peroxidase in the Side Effects of the Drugs

Ekaterina A. Korobkova,* William Ng, Abhishek Venkatratnam, Alicia K. Williams, Madina Nizamova, and Nikolay Azar

Science Department, John Jay College of Criminlal Justice, 445 W. 59th Avenue, New York, New York 10019

Received June 30, 2010

Studies show that tricyclic antidepressants prescribed for migraines, anxiety, and child enuresis have numerous adverse effects in living cells. One of the undesired outcomes observed under treatment with these drugs is DNA damage. However, the mechanisms underlying damage have yet to be elucidated. We performed *in vitro* studies of the DNA damage caused by four tricyclic antidepressants: imipramine, amitriptyline, opipramol, and protriptyline. We focused particularly on the DNA damage aided by peroxidases. As a model of a peroxidase, we used horseradish peroxidase (HRP). At pH 7, reactions of HRP with excess hydrogen peroxide and imipramine yielded an intense purple color and a broad absorption spectrum with the maximum intensity at 522 nm. Reactions performed between DNA and imipramine in the presence of H_2O_2 and HRP resulted in the disappearance of the DNA band. In the case of the other three drugs, this effect was not observed. Extraction of the DNA from the reaction mixture indicated that DNA is degraded in the reaction between imipramine and H_2O_2 catalyzed by HRP. The final product of imipramine oxidation was identified as iminodibenzyl. We hypothesize that the damage to DNA was caused by an imipramine reactive intermediate.

Introduction

Tricyclic antidepressants have been extensively used over the last several decades for the treatment of insomnia, headaches, depression, and childhood enuresis. These drugs can be very toxic not only if taken in overdosage but also under normally prescribed amounts. Antidepressants and their metabolites are potentially very reactive toward DNA in living cells. DNA presents many reactive rich sites; its bases and backbones are often targets for various chemicals present in the cell. The damage, if not repaired, can lead to very serious health issues, particularly inducing cancer (*1, 2*). Tricyclic antidepressants with their planar structures can insert between DNA bases, forming stacking complexes. For example, imipramine has been found to be a DNA intercalator (*3, 4*). The metabolism of antidepressants may lead to even more severe DNA damage, such as strand breaks (*5*).

The DNA damage caused by tricyclic antidepressants has been studied in cells, animals, and humans. Strand breaks, chromosome aberrations, and sister chromatid exchanges have been detected in cells exposed to imipramine and amitriptyline (*5, 6*). Mice studies revealed the decrease of marrow-mitotic division caused by imipramine and desipramine (*7*). DNA damage was also detected in a group of children treated with imipramine for nocturnal enuresis (*8*). The mechanisms underlying DNA damage caused by tricyclic antidepressants and their metabolites are not completely understood.

Recently, much interest has been drawn toward radical mediated DNA damage (*9*−*12*). There is also sufficient evidence of free radical formations due to the oxidation of drugs, carcinogens, and xenobiotics by peroxidases (*13*−*15*). The radicals formed during peroxidase catalysis are potentially harmful to the living cells, as they react with DNA, proteins, fatty acids, and other molecules (*16, 17*). These reactive intermediates may abstract a hydrogen atom from a ribose ring causing DNA cleavage or inter- and intramolecular cross-links. Molecules with an unpaired electron may also bind to DNA, producing stable covalent complexes (*18*). The resulting products prevent certain DNA processes from functioning normally.

We performed *in vitro* DNA damage studies of two high suicide-risk antidepressants, imipramine and amitriptyline (*19, 20*), and structurally related opipramol and protriptyline (Figure 1). As a model of peroxidase, we employed horseradish peroxidase (HRP). We attempted to correlate the DNA damage potency of the antidepressants with their structural characteristics. We performed comparative analysis of their DNA damage potency aided by hydrogen peroxide and HRP.

Experimental Procedures

Materials. Imipramine hydrochloride, purity ≥99% (Allentown, PA), amitriptyline hydrochloride, purity ≥98% (Allentown, PA), opipramol dihydrochloride, purity ≥98% (Saint Louis, MO), protriptyline hydrochloride, purity ≥99% (Saint Louis, MO), DNA type I from calf thymus (Allentown, PA), peroxidase from horseradish type VI, 250−330 units/mg (Allentown, PA), and hydrogen peroxide (Allentown, PA) were purchased from Sigma Aldrich. Wide range DNA marker, 16 fragments, 50−10,000 bp (Saint Louis, MO) was also purchased from Sigma Aldrich. Plasmid pBR322 (0.25 μg/μL, 4363 bp) purified from *E.coli* DH10B (Carlsbad, CA) was purchased from Invitrogen. PCI mixture, ratio 25:24:1, biotech grade, 1 M Tris buffer (pH 6.7), was purchased from Fisher Scientific (Fairlawn, NJ).

Reactions. The standard reaction mixture with calf thymus DNA contained (unless otherwise specified) 0.2 μM HRP, 13 μM per bp calf thymus DNA (~10 ng/μL), 500 μM antidepressant, and 500 μM H_2O_2 in Sorenson buffer (pH 7.0) containing 67 mM dibasic

* To whom correspondence should be addressed. Tel: 1-212-237-8064. E-mail: ekorobkova@jjay.cuny.edu.

10.1021/tx100221b
Published on Web 08/30/2010

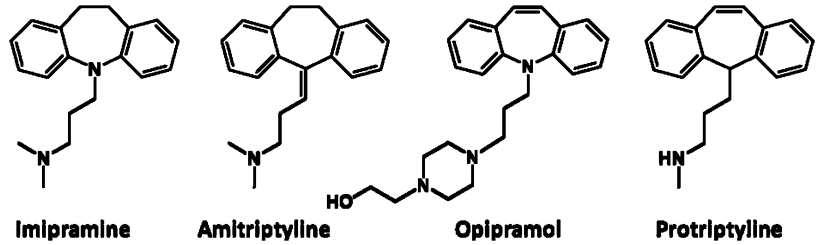

Figure 1. Structures of tricyclic antidepressants.

sodium phosphate and 67 mM monobasic potassium phosphate. The standard reaction mixture with pBR322 plasmid contained 0.2 μM HRP, 3 ng/μL (~5 μM per bp) plasmid, 500 μM antidepressant, and 500 μM H_2O_2 in 67 mM Sorenson buffer (pH 7.0). The volume of the reaction mixtures prepared for the 15-well gels was 10 μL; the volume of the reactions prepared for 8-well gels was 20 μL. The components were added in the order listed. All reaction mixtures were incubated at 37 °C for 1 h in a water bath.

Gel Electrophoresis. One percent agarose gels were prepared in TAE buffer. Electrophoresis was performed at 80 V for 120 min. In the case of 15-well gels, the loading samples contained 10 μL of the reaction mixture, and 1.1 μL of the 10× loading buffer. In the case of 8-well gels, the loading samples contained 20 μL of the reaction mixture, and 2.2 μL of the 10× loading buffer. The 10× loading buffer consisted of 50% glycerol, 0.25% bromophenol blue, and 0.25% xylene cyanole FF in TAE buffer. The gel was stained in ethidium bromide (0.5 μg/mL) for 20 min and then destained in distilled water for 20 min. The gel images were captured with a PerkinElmer Geliance 200 Imaging system.

PCI DNA Extraction Protocol. Forty microliters of DNA sample was taken in a 1.5 mL Eppendorf tube. Equal volume of phenol/chloroform/isoamyl alcohol (PCI, 25:24:1) was added to the tube. The two liquid layers (aqueous and organic) were mixed by flicking the tubes. The tubes were then centrifuged at 12,000 rpm for 5 min. The aqueous phase (upper layer) was carefully transferred to a clean centrifuge. To this tube, equal volume of chloroform was added. The two liquid layers (aqueous and organic) were mixed by flicking the tubes. The tubes were then centrifuged at 12,000 rpm for 5 min. The aqueous phase (upper layer) was carefully transferred to a clean centrifuge. The chloroform extraction procedure was repeated 7 times. The extracted samples were quantified with NanoDrop 2000C Spectrophotometer (Thermo Scientific).

Absorption Spectra of HRP. All UV−vis absorption spectra were recorded with Shimazu UV−visible Spectrophotometer, UV-1700. The original solution contained 10 μM HRP in 500 μL of 67 mM Sorenson buffer (pH 7.0). H_2O_2 stock solution of 0.5 mM was added to a final concentration of 10 μM, after which the spectrum of HRP-I was recorded. Antidepressants were added to a final concentration of 5−20 μM from the 0.5 mM stock solutions, after which the spectra of HRP-II and regenerated HRP were recorded. The temperature in the cuvette chamber was maintained at 20 °C. The reference cuvette contained 67 mM Sorenson buffer (pH 7.0). The concentration of HRP was calculated using the extinction coefficients at 404 nm of 102,000 M^{-1} cm^{-1} (*21*).

Gas Chromatography−Mass Spectrometry (GC-MS). Mass spectrometry data was acquired on an Agilent Technologies 7890A GC/MS instrument with 5975C Mass Selective Detector (MSD). NIST MS Search 2.0 MS Spectral library was supplied with the Agilent GC/MS instrument. The instrument was setup as follows.

Part I, GC. (a) Autosampler setup: 2 μL injections at fast speed setting with 7 s viscosity delay. (b) Injection port setup: splitless injection, front inlet, 250 °C; purge flow, 0.5 mL/min; purge time, 2 min; pressure, 10.523 psi; septum purge flow, 3 mL/min; gas saver on at 20 mL/min after 2 min. (c) Column: an HP-5MS column, 30 m × 25 mm × 0.25 μm film thickness; column He 5.0 gas flow, 1.0 mL/min at 7.37 psi. (d) Oven: oven initial temperature, 100 °C held for 0 min, at 8 °C/min ramp to 300 °C, held for 2 min; total run time, 27 min.

Part II, MS. (a) Transfer line: 300 °C isocratic. (b) MSD acquisition parameters: acquisition mode, scan; solvent delay, 2 min; EM offset, 0, EM voltage 965 was used. Scan parameters: low mass, 50.0; high mass, 800; threshold, 150. Sampling rate (2^n) was 2. MS Quad temperature, 150 °C; MS Source temperature, 230 °C.

Results

Reactions between DNA and Antidepressants. Reactions of antidepressants with DNA were performed in the presence and absence of HRP/H_2O_2. Antidepressants were imipramine, amitriptyline, opipramol, or protriptyline (Figure 1). Reaction mixtures were electrophoressed, and the gel images are shown in Figure 2. Reactions were performed with calf thymus DNA (Figure 2A) and digested plasmid pRB322 (Figure 2B). Reactions between DNA and the drugs showed a maintaining of the DNA band (Figure 2A and B, lanes 4−7). However, reactions between DNA and imipramine conducted in the presence of

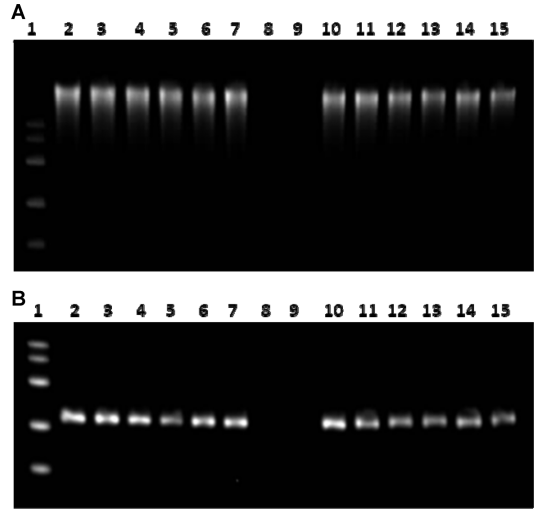

Figure 2. Agarose gel electrophoresis of reaction mixtures containing DNA and antidepressants. All reactions mixtures were incubated for 1 h at 37 °C. Concentrations of all drugs, HRP, and H_2O_2 were 0.5 mM, 0.2 μM, and 0.5 mM, respectively, in all reactions. The concentration of calf thymus DNA was 13 μM per bp in all reaction mixtures. The concentration of the digested plasmid was 3 ng/μL. (A) Reactions with calf thymus DNA. Lane 1, wide range DNA marker, 50−10,000 bp, 5 μL; lane 2, DNA only; lane 3, DNA and HRP/H_2O_2 (control reaction); lane 4, DNA and imipramine; lane 5, DNA and amitriptyline; lane 6, DNA and opipramol; lane 7, DNA and protriptyline; lanes 8 and 9, DNA, imipramine, and HRP/H_2O_2; lanes 10 and 11, DNA, amitriptyline, and HRP/H_2O_2; lanes 12 and 13, DNA, opipramol, and HRP/H_2O_2; lanes 14 and 15, DNA, protriptyline, and HRP/H_2O_2. (B) Reactions with digested plasmid pBR322. Lane 1, DNA marker, 5 μL; lane 2, plasmid only; lane 3, plasmid and HRP/H_2O_2; lane 4, plasmid and imipramine; lane 5, plasmid and amitriptyline; lane 6, plasmid and opipramol; lane 7, plasmid and protriptyline; lanes 8 and 9, plasmid, imipramine, and HRP/H_2O_2; lanes 10 and 11, plasmid, amitriptyline, and HRP/H_2O_2; lanes 12 and 13, plasmid, opipramol, and HRP/H_2O_2; lanes 14 and 15, plasmid, protriptyline, and HRP/H_2O_2.

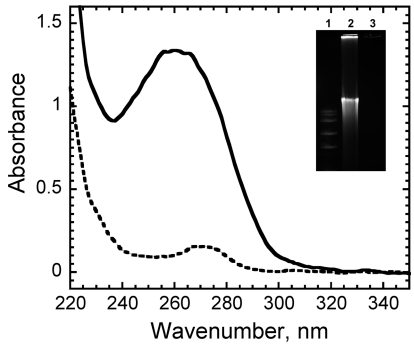

Figure 3. Quantitation of DNA extracted from the reaction mixture by PCI procedure (phenol/chloroform/isoamyl alcohol). Solid line, UV spectrum of sample extracted from a 40 μL solution containing 100 μM calf thymus DNA in water. Dashed line, UV spectrum of sample extracted from a 40 μL solution containing a reaction mixture: 100 μM calf thymus DNA, 2 μM HRP, 0.5 mM imipramine, and 5 mM H_2O_2 in water. (Inset) Agarose gel electrophoresis of DNA (lane 2) and DNA reaction mixture (lane 3). Gel electrophoresis was performed before the PCI extraction. Twenty microliters was loaded in each lane. Lane 1 is the wide range DNA marker, 50−10,000 bp.

HRP/H_2O_2 led to complete fading of the bands. (Figure 2A and B, lanes 8 and 9). No similar effect was observed with amitriptyline, opipramol, and protriptyline (Figure 2A and B, lanes 10−15). The control reaction, DNA + HRP + H_2O_2, resulted in the retention of the bands (Figure 2A and B, lane 3) suggesting an involvement of the drug in the DNA damaging process. The following control reactions were also performed and resulted with no loss of DNA: (1) DNA + antidepressant + H_2O_2 and (2) DNA + antidepressant + HRP (data not shown).

PCI DNA Extraction. DNA extraction was performed from samples containing (a) 100 μM DNA and (b) 100 μM DNA and imipramine incubated for 1 h at 37 °C in the presence of HRP/H_2O_2 in water. The extraction was performed using a Phenol/Chloroform/Isoamyl alcohol system. The detailed description of the procedure is shown in Experimental Procedures. Briefly, DNA was collected in the aqueous layer, and then the aqueous phase was purified with chloroform extractions. DNA was finally quantified with the NanoDrop spectrophotometer, and the results are shown in Figure 3. The control experiment (Figure 3, solid line) shows the UV spectrum of DNA extracted from the solution using the procedure described above. The absorbance of 1.3 at λ_{max}= 260 nm corresponds to a DNA concentration of 100 μM with an extinction coefficient for calf thymus DNA of 12,824 M(bp)$^{-1}$ cm^{-1} (*22*). The dashed line in Figure 3 shows the UV spectrum of the sample collected from the reaction mixture initially containing 100 μM DNA. DNA that was originally present in the solution disappeared from the sample in the course of the reaction as indicated by the absence of the peak at 260 nm. A peak at 270 nm is due to the remaining phenol. Gel electrophoresis was also performed, and the results are shown in the inset of Figure 3. This experiment combined with the gel electrophoresis studies shown in Figure 2 indicates that DNA degrades in the presence of imipramine, HRP, and H_2O_2.

Absorption Spectrophotometry Studies. The UV−vis absorption spectra were recorded for native and modified HRP. The catalytic cycle of HRP is shown in Scheme 1. In this scheme, HRP (native enzyme) is converted to the oxidized form HRP-I by hydrogen peroxide. The reactions HRP-I → HRP-II and HRP-II → HRP proceed through the abstraction of electrons from the drug molecules resulting in the formation of free radicals. In general, the oxidizing agent can be any organic peroxidase.

Scheme 1. Catalytic Cycle of HRP

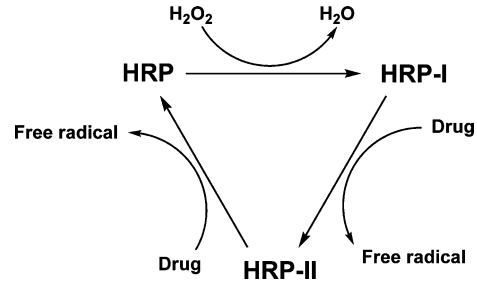

UV spectra of native HRP and its oxidized forms are shown in Figure 4A−D. Line a represents the spectrum of native HRP (∼10 μM). One equivalent of H_2O_2 was added to a brown solution of HRP with an appearance of a light green color. Line b represents the spectrum of HRP oxidized by H_2O_2, which is consistent with the spectrum recorded for HRP-I (*23*). The spectrum shifted toward the longer wavelengths, and the intensity of the absorbance decreased significantly. These observations are in agreement with the other studies (*24, 25*).

The addition of one equivalent of imipramine or half equivalent of opipramol to the solution of HRP-I led to the UV−vis spectrum characteristic for HRP-II (*23*) with a significant increase in signal compared to that of HRP-I, and the maximum peak shifted to a longer wavelength with respect to the spectrum of native HRP (Figure 4A and C, line c). The addition of another equivalent of imipramine or another half equivalent of opipramol resulted in the regeneration of the spectrum characteristic for native HRP (Figure 4A and C, line d). The addition of 1 and 10 equivalents of amitriptyline or protroptyline to the solution of HRP-I did not lead to a spectrum change (Figure 4B and D, lines c and d). This suggests that amitriptyline and protriptyline do not react with the oxidized prosthetic group of HRP. The slight increase in the intensity is associated with the instability of the HRP-I, which is reduced spontaneously by solution impurities (*26*). The addition of either antidepressant to a solution of native HRP not containing H_2O_2 demonstrated no effect on the spectrum.

Both imipramine and opipramol proved to be substrates for HRP. However, DNA degradation was observed only in the presence of imipramine (Figure 2A and B, lanes 8 and 9; Figure 3). We performed more detailed studies of the spectra appearing in the reaction of imipramine with HRP/H_2O_2.

The addition of excess imipramine to the mixture of HRP and H_2O_2 yielded a spectrum with the maximum absorption at 522 nm. Figure 5A shows the UV−vis absorption spectrum recorded from the mixture containing 0.2 μM HRP, 500 μM H_2O_2, and 500 μM imipramine in 2 mM phosphate buffer (pH 7). The intensity of the spectrum increased for approximately 1 h and 20 min, after which it decreased showing a new absorption maximum at 340 nm. The color of the solution proceeded from pink to light purple and to brown as the absorbance at 522 nm increased. A reaction between imipramine and HRP/H_2O_2 performed in water yielded a similar spectrum with a peak at 522 nm (data not shown). Mixing imipramine with H_2O_2 or HRP alone did not yield a purple color or the corresponding absorption spectrum.

The same experiments were repeated with different pH values, and the results are shown in Figure 5B, C, and D. The maximum of the spectrum shifted to longer wavelengths as the pH decreased. At pH 5.5, the color of the solution evolved from dark blue-brown (λ_{max} = 560 nm) to brown

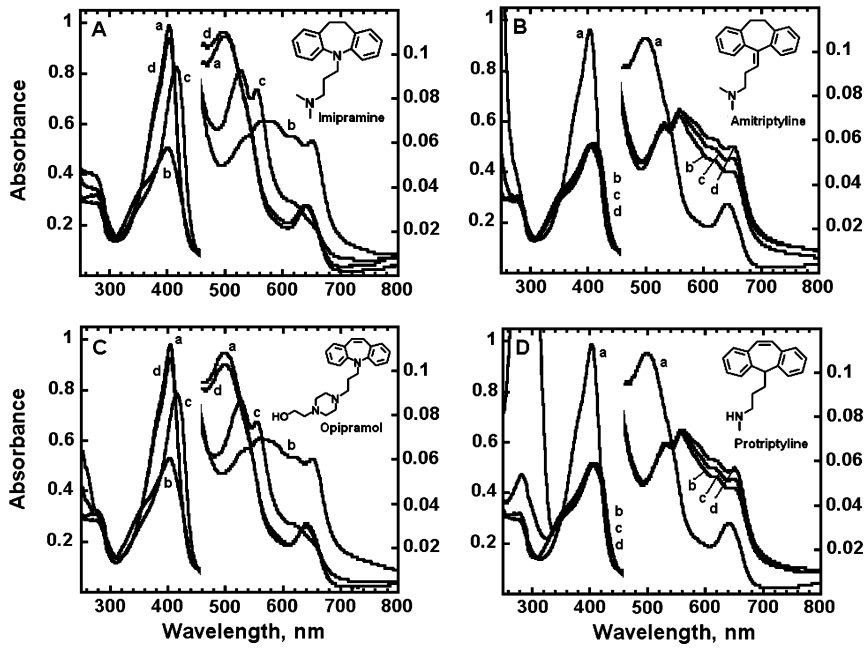

Figure 4. UV−vis absorption spectra of HRP treated with H_2O_2 and antidepressants. (A) Line a, native HRP 10 μM; line b, HRP with one equivalent of H_2O_2; line c, spectrum recorded after the addition of 1 equivalent of imipramine; line d, after the addition of 2 equivalents of imipramine. (B) Line a, 10 μM native HRP; line b, HRP with one equivalent of H_2O_2; line c, after the addition of 1 equivalent of amitriptyline; line d, after the addition of 10 equivalents of amitriptyline. (C) Line a, 10 μM native HRP; line b, HRP with one equivalent of H_2O_2; line c, after the addition of 1 half equivalent of opipramol; line d, after the addition of 1 equivalent of opipramol. (D) Line a, 10 μM native HRP; line b, HRP with one equivalent of H_2O_2; line c, after the addition of 1 equivalent of protriptyline; line d, after the addition of 10 equivalents of protriptyline.

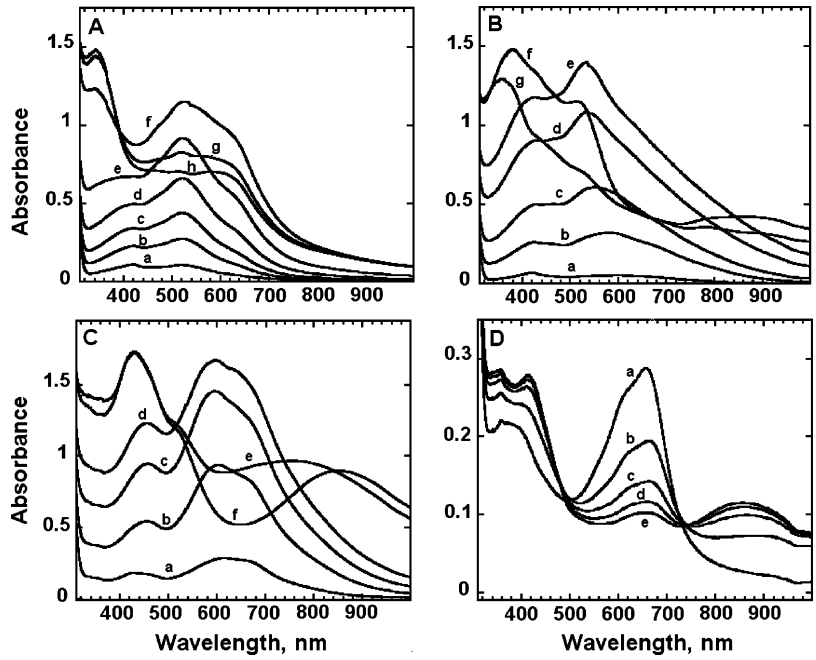

Figure 5. UV−vis absorption spectra of reaction mixtures containing HRP and excess of H_2O_2 and imipramine. (A) Phosphate buffer (2 mM, pH 7). Concentrations of HRP, H_2O_2, and imipramine are 0.2 μM, 0.5 mM, and 0.5 mM, respectively. Spectrum a, 3 min after mixing the reagents; spectrum b, 6 min after mixing; spectrum c, 10 min; spectrum d, 17 min; spectrum e, 29 min; spectrum f, 1 h 17 min; spectrum g, 1 h and 23 min; spectrum h, 1 h and 45 min. (B) Phosphate buffer (2 mM, pH 5.5). Concentrations of HRP, H_2O_2, and imipramine are 0.2 μM, 0.5 mM, and 0.5 mM, respectively. Spectrum a, 2 min after mixing the reagents; spectrum b, 5 min after mixing; spectrum c, 7 min; spectrum d, 17 min; spectrum e, 24 min; spectrum f, 1 h and 24 min; spectrum g, 3 h and 33 min. (C) Phosphate buffer (2 mM, pH 4.7). Concentrations of HRP, H_2O_2, and imipramine are 0.2 μM, 0.5 mM, and 0.5 mM, respectively. Spectrum a, recorded after mixing the reagents; spectrum b, 2 min after mixing; spectrum c, 4 min; spectrum d, 6 min; spectrum e, 14 min; spectrum f, 30 min. (D) Phosphate buffer (2 mM, pH 2). Concentrations of HRP, H_2O_2, and imipramine are 2 μM, 1 mM, and 1 mM, respectively. Spectrum a, recorded after mixing the reagents; spectrum b, 2 min after mixing; spectrum c, 4 min; spectrum d, 6 min; spectrum e, 8 min.

and to light orange (Figure 5B). At pH 4.7, the blue solution (λ_{max} = 600 nm) turned red-brown in the course of the reaction (Figure 5C). At pH 2, the blue solution (λ_{max}= 650 nm) turned green with the maximum intensity decreasing, yielding a new peak at ~400 nm (Figure 5D). Borg (*27*) recorded similar spectra in imipramine reaction mixtures with ferric salts, ceric ion, and HRP/H_2O_2 in acid. Sakurai et al. (*28*) observed the blue spectrum in the reaction of imipramine and vanadate ion. In both studies, the blue color converted to green spontaneously. EPR (electron paramagnetic reso-

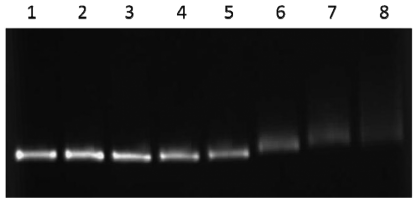

Figure 6. Drug concentration dependence study. Gel electrophoresis of the reaction mixtures containing plasmid DNA, imipramine, and HRP/H_2O_2. All reaction mixtures contained 3 ng/μL (~5 μM) of digested pBR322 plasmid, 0.2 μM HRP, and 0.5 mM H_2O_2. Concentration of imipramine varied as follows: lane 1, none; lane 2, 2 μM; lane 3, 5 μM; lane 4, 8 μM; lane 5, 11 μM; lane 6, 14 μM; lane 7, 17 μM; lane 8, 20 μM. All reaction mixtures were incubated for 1 h in a 37 °C water bath.

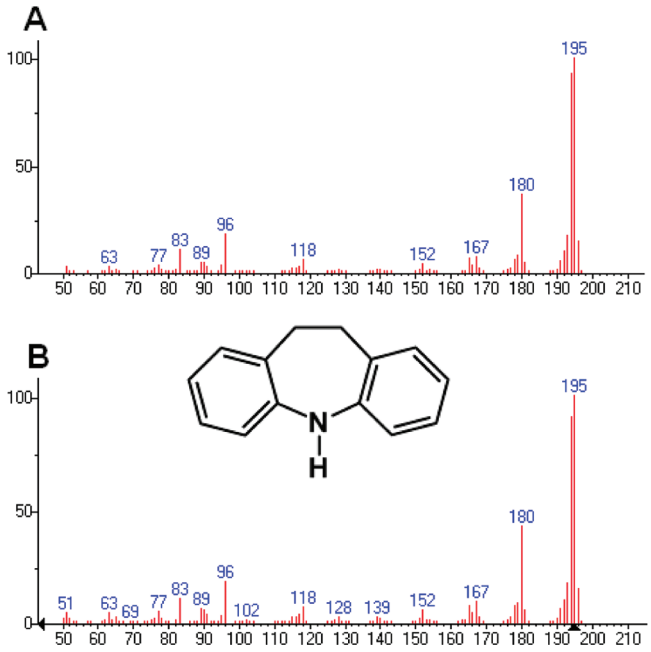

Figure 7. Mass spectral analysis of the imipramine oxidation product. (A) Mass spectrum of the major product formed in the reaction of imipramine with HRP/H_2O_2. The GC retention time of the compound was 16 min. (B) Matching spectrum from the library and structure of 10,11-dihydro-5*H*-dibenz[*b*,*f*]azepine (iminodibenzyl).

nance) spectra were recorded from the reaction mixtures and associated with a transitory free radical from imipramine (*27, 28*).

Concentration Dependence Studies. Reactions between plasmid DNA and imipramine were performed in the presence of HRP/H_2O_2 with the drug concentration ranging from 2 μM to 20 μM (10 to 100 mol equiv of HRP). The reaction mixtures were analyzed with gel electrophoresis, and the image is shown in Figure 6. It can be seen that the band intensity faded as the drug concentration increased. At imipramine concentrations greater than 30 μM, the DNA band disappeared completely.

Mass Spectral Analysis. Overnight incubation of the reaction mixture containing imipramine, H_2O_2, and HRP at room temperature or 1 h of incubation at 37 °C resulted in the formation of a brown precipitate, which dissolved freely in acetonitrile. The sample was analyzed with GC-MS. The retention time of a major peak was 16 min. The mass spectrum is shown in Figure 7A. The spectrum matched that of iminodibenzyl (Figure 7B). The systematic name of the compound is 10,11-dihydro-5*H*-dibenz[*b*,*f*]azepine.

Scheme 2. Resonance Structures of Imipramine[a]

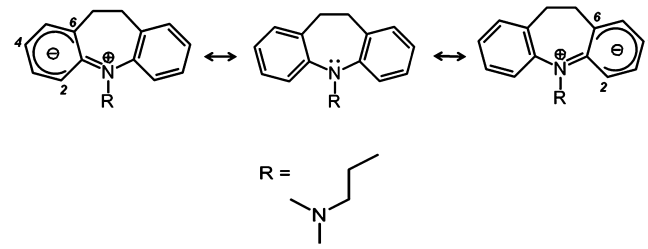

[a] Numbers, 2, 4, and 6 indicate the location of the negative charge on the carbon atoms of the benzene rings.

Discussion

Analysis of the reaction mixtures containing calf thymus genomic DNA or digested plasmid pBR322, imipramine, and HRP/H_2O_2 resulted in the disappearance of the DNA band from the gel images (Figure 2A and B, lanes 8 and 9; Figure 3, inset). The PCI extraction of calf thymus DNA from the reaction mixtures containing imipramine and the HRP/H_2O_2 oxidation system showed that DNA degrades in the reaction (Figure 3, dashed line). The DNA damage is probably caused by the reactive intermediate formed during electron transfer from imipramine to the oxidized forms of HRP, HRP-I, and HRP-II.

Oxidation−reduction cycle of HRP proceeds through the formation of HRP-I and HRP-II (Scheme 1). The structure of the active sites of native and oxidized forms has been characterized for some peroxidases. The prosthetic group of the native peroxidase contains iron in its ferric state. In HRP-I, the iron is in the ferryl state in the iron-oxo complex (*23*). Moreover, HRP-I is characterized by the presence of the radical cation, which rests on the porphyrine ring of the heme (*29*) or in an amino acid residue (*30*). The HRP-II complex of peroxidases contains a fully covalent ferryl-oxo complex (*23*).

Spectroscopy studies of HRP were performed to study the processes that affect DNA when antidepressants are present with HRP/H_2O_2. The UV−vis absorption spectra of HRP and its oxidized forms have been well characterized (*23*). The addition of imipramine, amitriptyline, opipramol, and protriptyline to the HRP-I solution led to different effects (Figure 4A−D). In the case of amitriptyline or protriptyline, the addition of excess amounts of the drug to the solution of HRP-I resulted in almost no spectrum change (Figure 4B and D). However, in the case of imipramine or opipramol, the consecutive addition of small aliquots (within the 2 equivalents of HRP) of the drug led to a spectrum characteristic of the HRP-II compound (Figure 4A and C, line c) and a spectrum, which coincided with that of the native HRP (Figure 4A and C, line d).

We envision that the difference in reactivity of the drugs with HRP-I is associated with their nucleophilic properties. The overlapping of the free electron pair on the N-atom of imipramine may lead to an increase in nucleophilicity as a result of negative charge delocalization on the benzene rings. This can be rationalized through the resonance structures as shown in Scheme 2. Both amitripyline and protriptyline do not have a nitrogen atom bridging the aromatic rings and consequently do not display this increased nucleophilicity (Figure 1). The localization of the negative charge on the benzene rings of the drug can also facilitate the abstraction of the electron, therefore increasing its reduction potential and aiding the reactions, HRP-I → HRP-II and HRP-II → HRP. As the enzyme carries on through a large number of cycles, radicals may generate (Scheme 1).

The addition of the excess of imipramine and H_2O_2 to the HRP yielded a purple color which intensified with time. At pH

7, a spectrum with a strong absorption maximum at 522 nm appeared (Figure 5A). The same reaction conducted at pH 2 resulted in the appearance of a spectrum with $\lambda_{max} = 650$ nm (Figure 5D). The spectrum was very unstable at pH 2 and disappeared in 4 min. These observations are consistent with the studies of imipramine mixtures with ceric ion and vanadyl ion. EPR of transitory imipramine radical was detected in these reactions (*27, 28*). In the present work, the formation of the imipramine radical is supported by stoichiometry. HRP-I → HRP-II transitions occur through the abstraction of one electron from the reducing agent (*26*). In the case of imipramine, the HRP-II was produced after the addition of one HRP equivalent of the drug to the HRP-I solution (Figure 4A). This indicates that each imipramine molecule loses one electron in this step, suggesting the formation of an unpaired-electron species.

Reactions between aromatic amines and hydroperoxides have been studied in the presence of peroxidases; the appearance of purple color was associated with the formation of the radical cation. Griffin and co-workers (*31*) detected free radicals of aminopyrine formed by microsomal cytochrome P450 in the presence of cumene hydroperoxide. Free radicals of aminopyrine have also been observed in the lipoxygenase/H_2O_2 system (*32*). Various phenothiozines have been shown to produce radical cations in the presence of HRP and H_2O_2, the maximum wavelength varying between 500 and 630 nm (*33, 34*). Crystal violet has been shown to produce free radicals in the reaction with H_2O_2 catalyzed by HRP (*35*).

The final product in the reaction between imipramine and HRP/H_2O_2 was identified as a dealkylated imipramine, iminodibenzyl (Figure 7C). The N-dealkylation mechanism was also proposed for aromatic amines, aminopyrine (*32*) and crystal violet (*35*). Hufford and co-workers identified iminodibenzyl as an imipramine metabolite using fungal organisms (*36*).

Our experiments showed that oxidation of imipramine catalyzed with HRP leads to the degradation of DNA (Figure 2A and B, lanes 8 and 9; Figure 3). Radical induced DNA cleavage has been studied extensively with respect to OH radicals formed in Fenton reactions (*10, 11*). DNA cleavage by OH radicals has biotechnological applications (*11*). The antidepressant, 2-phenylethylhydrazine, was shown to induce DNA strand breaks through the metabolically generated carbon-centered radicals (*37*). The studies related to the interactions between DNA and nitrogen-centered radicals, however, are very limited. Murata and co-workers showed that the N-centered radical formed from acrylonitrile enhances DNA damage produced by H_2O_2 and Cu(II) (*12*).

Genotoxicity of imipramine has been assessed in various systems, and it has been found to cause significant DNA damage in mice (*7*), human lymphocytes (*6, 8*), and C6 rat glioma cells (*5*). Saxena and Ahuja performed comparative studies of genotoxicity of imipramine and amitriptyline in human lymphocyte cultures (*6*). They found that amitriptyline caused chromosome damage at concentrations significantly greater than those attained in patients under normal therapy. However, imipramine exhibited a substantial increase in chromosome aberrations at the upper level of therapeutic doses, 500 ng/mL (~2 μM). Our studies indicate that imipramine may cause significant DNA degradation at concentrations of 2−5 μM (Figure 6). Amitriptyline shows no effect on DNA at the same conditions. The damage caused by imipramine is associated with the formation of a very reactive imipramine intermediate.

Acknowledgment. This work was supported by a PSC-CUNY grant and the PRISM program at John Jay College of Criminal Justice. We cordially thank Professor Nathan Lents for technical help and valuable discussions. We are grateful to Professor Marcel Roberts for the help with the manuscript, Dr. Steffen Jockusch for his constructive comments, and Dr. Arkadiy Bolshov for a number of useful conversations. We also thank anonymous referees for their many constructive remarks on the original version of the manuscript.

References

(1) Yarosh, D. B. (1985) The role of O6-methylguanine-DNA methyltransferase in cell survival, mutagenesis, and carcinogenesis. *Mutat. Res. 145*, 1–16.
(2) Friedberg, E. C. (2001) How nucleotide excision repair protects against cancer. *Nature Rev. Cancer 1*, 22–33.
(3) Snyder, R. D., and Arnone, M. R. (2002) Putative identification of functional interactions between DNA intercalating agents and topoisomerase II using the V79 *in vitro* micronucleus assay. *Mutat. Res. 503*, 21–35.
(4) Snyder, R D., Ewing, D. E., and Hendry, L. B. (2004) Evaluation of DNA intercalation potential of pharmaceutical and other chemicals by cell-based and three-dimensional computational approaches. *Environ. Mol. Mutagen. 44*, 163–173.
(5) Slamon, N. D., Ward, T. H., Butler, J., and Pentreath, V. W. (2001) Assessment of DNA damage in C6 glicoma cells after antidepressant treatment using an alkaline comet assay. *Arch. Toxicol. 75*, 243–250.
(6) Saxena, R., and Ahuja, Y. R. (1988) Genotoxicity evaluation of the tricyclic antidepressants amitriptyline and imipramine using human lymphocyte cultures. *Environ. Mol. Mutagen. 12*, 421–430.
(7) Madrigal-Bujaidar, E., Madrigal-Santillán, E. O., Alvarez-Gonzalez, I., Baez, R., and Pilar Marquez, P. (2008) Micronuclei induced by imipramine and desipramine in mice: a subchronic study. *Basic Clin. Pharmacol. Toxicol. 103*, 569–573.
(8) Dungaros, R., Turkbay, T., Surer, I., Gok, F., Denli, M., and Baltaci, V. (2002) DNA damage in children treated with imipramine for primary nocturnal enuresis. *Pediatr. Int. 44*, 617–621.
(9) Yamamoto, K., and Kawanishi, S. (1992) Site-specific DNA damage by phenylhydrazine and phenelzine in the presence of Cu(II) ion or Fe(III) complexes: roles of active oxygen species and carbon radicals. *Chem. Res. Toxicol. 5*, 440–446.
(10) Balasubramanian, B., Pogozelski, W. K., and Tullius, T. D. (1998) DNA strand breaking by the hydroxylradical is governed by the accessible surface areas of the hydrogen atoms on the DNA back bone. *Proc. Natl. Acad. Sci.U.S.A. 95*, 9738–9743.
(11) Henle, E. S., Han, Z., Tang, N., Rai, P., Luo, Y., and Linni, S. (1999) Sequence-specific DNA cleavage by Fe^{2+}-mediated Fenton reactions has possible biological implications. *J. Biol. Chem. 274*, 962–971.
(12) Murata, M., Ohnishi, S., and Kawanishi, S. (2001) Acrylonitrile enhances H_2O_2-mediated DNA damage via nitrogen-centered radical formation. *Chem. Res. Toxicol. 14*, 1421–1427.
(13) Eghbal, M. A., Tafazoli, S., Pennefather, P., and O'Brien, P. J. (2004) Peroxidase catalyzed formation of cytotoxic prooxidant phenothiazine free radicals at physiological pH. *Chem.-Biol. Interact. 151*, 43–51.
(14) Ritter, C. L., Malejka-Giganti, D., and Polnaszek, C. F. (1983) Cytochrome c/H_2O_2-mediated one electron oxidation of carcinogenic N-fluorenylacetohydroxamic acids to nitroxyl free radicals. *Chem.-Biol. Interact. 46*, 317–334.
(15) O'Brien, P. J. (2000) Peroxidases. *Chem.-Biol. Interact. 129*, 113–139.
(16) O'Brien, P. J. (1988) Radical formation during the peroxydase catalyzed metabolism of carcinogens and xenobiotics: The reactivity of these radicals with GSH, DNA, and unsaturated lipid. *Free Radical Biol. Med. 4*, 169–183.
(17) Miura, T., Muraoka, S., and Fujimoto, Y. (2001) Inactivation of creatine kinase during the interaction of indomethacin with horseradish peroxidase and hydrogen peroxide: Involvement of indomethacin radicals. *Chem.-Biol. Interact. 134*, 13–25.
(18) O'Brien, P. J. (1985) Free-radical-mediated DNA binding. *Environ. Health. Perspect. 64*, 219–232.
(19) Mittmann, N. M., Lui, B. A., Bparm, M. I., Bradley, C. A., Pless, R., Shear, N. H., and Einarson, T. R. (1997) Drug-related mortality in Canada (1984-1994). *Pharmacoepidemiol. Drug Saf. 6*, 157–168.
(20) Caplan, Y. H., Ottinger, W. E., Jongsei, P., and Smith, T. D. (1985) Drug and chemical related deaths: Incidence in the state of Maryland. *J. Forensic Sci. 30*, 1012–1021.
(21) Song, H.-Y., Yao, J.-H., Liu, J.-Z., Zhou, S.-J., Xiong, Y.-H., and Ji, L.-N. (2005) Effects of phthalic anhydride modification on horseradish peroxidase stability and structure. *Enzyme Microb. Technol. 36*, 605–611.
(22) Suh, D., and Chaires, J. B. (1995) Criteria for the mode of binding of DNA binding agents. *Bioorg. Med. Chem. 3*, 723–728.

(23) Dunford, H. B., and Stillman, J. S. (1976) On the function and mechanism of action of peroxidases. *Coord. Chem. Rev. 19*, 187–251.
(24) Aitkem, S. M., Ouellet, M., Percival, M. D., and English, A. M. (2003) Mechanism of Horseradish peroxidase inactivation by benzhydrazide: a critical evaluation of arylhydrazides as peroxidase inhibitors. *Biochem. J. 375*, 613–621.
(25) Ator, M., and Ortiz de Montellano, P. R. (1987) Protein control of prosthetic heme reactivity. *J. Biol. Chem. 262*, 1542–1551.
(26) Ortiz de Montellano, P. R. (1986) In *Cytochrome P-450: Structure, Mechanism and Biochemistry* (Ortiz de Montellano, R. P. Ed.) Plenum Press, New York.
(27) Borg, D. C. (1965) Free radicals from imipramine. *Biochem. Pharmacol. 14*, 115–120.
(28) Saakurai, H., and Goda, T. (1983) Formation of imipramine free radical and vanadyle ion in the reaction of imipramine and pentavalent vanadium ion. *Inorg. Chim. Acra 78*, L33–L34.
(29) Edwards, S. L., Raag, R., Wariishi, H., Gold, M. H., and Poulos, T. L. (1993) Crystal structure of lignin peroxidase. *Proc. Natl. Acad. Sci.U.S.A. 90*, 750–754.
(30) Sivaraja, M., Goodin, D. B., Smith, M., and Hoffman, B. M. (1989) Identification by ENDOR of Trp191 as the free-radical site in cytochrome c peroxidase compound ES. *Science 245*, 738–740.
(31) Griffin, B. W., Marth, C., Yasukochi, Y., and Masters, B. S. S. (1980) Radical mechanism of aminopyrine oxidation by cumene hydroperoxide catalyzed by purified liver microsomal cytochrome P-450. *Arch. Biochem. Biophys. 205*, 543–553.
(32) Perez-Gilabert, M., Sanchez-Ferrer, A., and Garcia-Carmona, F. (1997) Oxidation of aminopyrine by the hydroperoxidase activity of lipoxygenase: a new proposed mechanism of N-demethylation. *Free Radical Biol. Med. 23*, 548–555.
(33) Vazquez, A., Tudela, J., Varon, R., and Garcia-Canovas, F. (1991) Determination of the molar absorptivities of phenothiazine cation radicals generated by oxidation with hydrogen peroxide/peroxidase. *Anal. Biochem. 202*, 245–248.
(34) Sackett, P. H., Mayausky, J. S., Smith, T., Kalus, S., and McCreery, R. L. (1981) Side-chain effects on phenothiazine cation radical reactions. *J. Med. Chem. 24*, 1342–1347.
(35) Gadelha, F. R., Hanna, P. M., Mason, R. P., and Docampo, R. (1992) Evidence for free radical formation during horseradish peroxidase-catalyzed N-demethylation of crystal violet. *Chem.-Biol. Interact. 85*, 35–48.
(36) Hufford, C. D., Capiton, G. A., Clark, A. M., and Baker, J. K. (1981) Metabolism of imipramine by microorganisms. *J. Pharm. Sci. 70*, 151–155.
(37) Saez, G., Thornalley, P. J., Hill, H. A. O., Hems, R., and Bannister, J. V. (1982) The production of free radicals during the authoxidation of cysteine and their effect on isolated rat hepatocytes. *Biochim. Biophys. Acta 719*, 24–31.

TX100221B